



OprF Impacts *Pseudomonas aeruginosa* Biofilm Matrix eDNA Levels in a Nutrient-Dependent Manner

Erin K. Cassin, ^a Sophia A. Araujo-Hernandez, ^a Dena S. Baughn, ^a Melissa C. Londono, ^a Daniela Q. Rodriguez, ^a Natalie S. Al-Otaibi, ^b Aude Picard, ^a Julien R. C. Bergeron, ^c Doo Shan Tseng ^a

^aSchool of Life Sciences, University of Nevada Las Vegas, Las Vegas, Nevada, USA

ABSTRACT The biofilm matrix is composed of exopolysaccharides, eDNA, membrane vesicles, and proteins. While proteomic analyses have identified numerous matrix proteins, their functions in the biofilm remain understudied compared to the other biofilm components. In the Pseudomonas aeruginosa biofilm, several studies have identified OprF as an abundant matrix protein and, more specifically, as a component of biofilm membrane vesicles. OprF is a major outer membrane porin of P. aeruginosa cells. However, current data describing the effects of OprF in the P. aeruginosa biofilm are limited. Here, we identify a nutrient-dependent effect of OprF in static biofilms, whereby $\Delta oprF$ cells form significantly less biofilm than wild type when grown in media containing glucose or low sodium chloride concentrations. Interestingly, this biofilm defect occurs during late static biofilm formation and is not dependent on the production of PQS, which is responsible for outer membrane vesicle production. Furthermore, while biofilms lacking OprF contain approximately 60% less total biomass than those of wild type, the number of cells in these two biofilms is equivalent. We demonstrate that P. aeruginosa ΔoprF biofilms with reduced biofilm biomass contain less eDNA than wild-type biofilms. These results suggest that the nutrient-dependent effect of OprF is involved in the maintenance of P. aeruginosa biofilms by retaining eDNA in the matrix.

IMPORTANCE Many pathogens form biofilms, which are bacterial communities encased in an extracellular matrix that protects them against antibacterial treatments. The roles of several matrix components of the opportunistic pathogen *Pseudomonas aeruginosa* have been characterized. However, the effects of *P. aeruginosa* matrix proteins remain understudied and are untapped potential targets for antibiofilm treatments. Here, we describe a conditional effect of the abundant matrix protein OprF on late-stage *P. aeruginosa* biofilms. A $\Delta oprF$ strain formed significantly less biofilm in low sodium chloride or with glucose. Interestingly, the defective $\Delta oprF$ biofilms did not exhibit fewer resident cells but contained significantly less extracellular DNA (eDNA) than wild type. These results suggest that OprF is involved in matrix eDNA retention in biofilms.

KEYWORDS OprF, biofilm matrix proteins, eDNA, nutrient-dependent, biofilm maintenance

iofilms are aggregates of bacterial cells encased in a self-produced extracellular matrix. The matrix protects resident cells from external assaults and is composed of exopoly-saccharides, extracellular DNA (eDNA), membrane vesicles, and proteins (1). Many studies have reported the effects of exopolysaccharides, eDNA, and membrane vesicles on biofilm function. However, relatively few have investigated the roles of biofilm matrix proteins, even though matrix proteins have been suggested to play many vital functions in the biofilm (2, 3). Since the late 2000s, researchers have used proteomic approaches to identify biofilm matrix proteins and gain insight into their roles, including several studies in the model

Editor George O'Toole, Geisel School of Medicine at Dartmouth

Copyright © 2023 Cassin et al. This is an openaccess article distributed under the terms of the Creative Commons Attribution 4.0

Address correspondence to Boo Shan Tseng, boo.tseng@unlv.edu.

The authors declare no conflict of interest.

Received 1 March 2023 Accepted 23 May 2023

^bDepartment of Biological Sciences, Birkbeck, University of London, London, United Kingdom

cRandall Centre for Cell and Molecular Biophysics, King's College London, London, United Kingdom

biofilm organism *Pseudomonas aeruginosa*. Four different studies have identified OprF as an abundant matrix protein (4–7). Additionally, homologs of *P. aeruginosa* OprF have been identified in biofilm matrices of other organisms (8–10).

Within the *P. aeruginosa* biofilm, two populations of OprF protein exist: cell associated and matrix associated. In its more established cell-associated role, OprF is an OmpA family member and the major nonspecific porin in *P. aeruginosa*, where it facilitates diffusion across the outer membrane (11). Multiple studies have examined biofilm formation after mutation of *oprF* or *ompA*, which eliminates both the cell- and matrix-associated protein pools (12–14). However, the impact of OprF and its OmpA homologs on biofilm formation is somewhat conflicting and may depend on conditions, such as oxygen or nutrient availability (15). One study shows that under aerobic conditions, a *P. aeruginosa oprF* interruption mutant produces twice as much biofilm as the parental strain (13). This result conflicts with a separate study in which an *oprF* mutant produced less biofilm when grown under anaerobic conditions (12). Furthermore, the OprF homolog OmpA, which is abundant in *Escherichia coli* biofilms (16), increases biofilm formation on hydrophobic surfaces (17). Mirroring this effect, in the pathogen *Acinetobacter baumannii*, *ompA* mutants are deficient in biofilm formation on abiotic surfaces and have decreased attachment to host cells (18). Together, these data suggest that OprF may play an important role in biofilm function.

Within the biofilm matrix, OprF is highly abundant in membrane vesicles, which are a major matrix component involved in biofilm structure and cell-to-cell signaling (5, 19). Two membrane vesicle synthesis pathways have been established: the bilayer couple model, which produces outer membrane vesicles (OMVs), and the explosive cell lysis model, which results in membrane vesicles (20, 21). Interestingly, OprF has been suggested to play a role in OMV production via the bilayer couple model. An OprF mutant overproduces OMVs relative to wild-type cells due to its overproduction of the quorum-sensing signal PQS (22). Since increased production of PQS and OMVs is correlated with biofilm dispersal (23), OprF may be important for this stage of the biofilm life cycle. However, the role of vesicle-associated OprF in the biofilm is currently unknown (11).

Here we identified a nutrient-dependent biofilm defect in $\Delta oprF$ strains of P. aeruginosa. Upon dissection of the medium components, we found that $\Delta oprF$ biofilm formation was significantly reduced in the presence of glucose or low sodium chloride concentrations without affecting overall bacterial growth. The biofilm defect in the absence of OprF occurs during late-stage biofilm development and is not dependent on PQS production. Interestingly, we observed equivalent numbers of cells in wild-type biofilms and $\Delta oprF$ biofilms (that have reduced biofilm biomass). However, there was a significant reduction in eDNA in $\Delta oprF$ biofilms grown in media containing glucose and low sodium chloride. Together, our data suggest that OprF is involved in the retention of eDNA during biofilm maintenance under certain growth conditions.

RESULTS

ΔoprF cells exhibit a nutrient-dependent biofilm defect. Since OprF is an abundant *P. aeruginosa* matrix protein (5, 6), we tested the effect of deleting *oprF* on biofilm formation. We deleted *oprF* from *P. aeruginosa* PAO1 and confirmed via whole-genome sequencing that our engineered deletion allele was the only difference between this strain and the parental strain. We also inserted an arabinose-inducible *oprF* at a neutral site in the chromosome in the $\Delta oprF$ background. This strain expressed OprF at levels similar to wild type upon addition of 0.5% arabinose but not in the absence of inducer (Fig. S1 in the supplemental material). Using standard 24-h microtiter biofilm assays (24), we compared the $\Delta oprF$ biofilm formed in two common growth media: tryptic soy broth (TSB) and lysogeny broth (LB). While forming more biofilm than the exopolysaccharide-deficient $\Delta pslD$ negative-control strain in both media, $\Delta oprF$ formed 57.3 \pm 3.8% SD (n = 3; P < 0.05, ANOVA with *post hoc* Bonferroni test) less biofilm than wild type in TSB, but an equivalent amount of biofilm to wild type in LB (Fig. 1A). This difference in biofilm formation was not due to growth rate differences in these media (Fig. S2) or major differences in cell size or morphology (Fig. S3), and the biofilm defect was partially complemented in the inducible *oprF*

Month YYYY Volume XX Issue XX

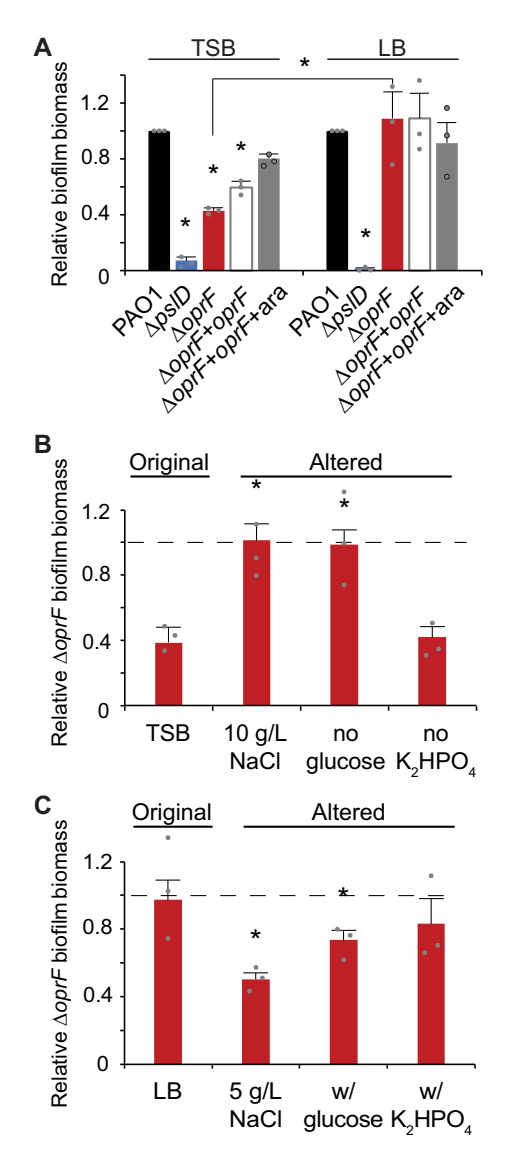


FIG 1 Δ*oprF* forms less biofilm in TSB than in LB, due to lower sodium chloride concentration and presence of glucose. (A) 24-h static microtiter biofilm assays of *P. aeruginosa* PAO1 (wild type [WT]; black), $\Delta psID$ (blue), $\Delta oprF$ (red), and a $\Delta oprF$ $attTn7::P_{BAD}-oprF$ restoration strain ($\Delta oprF + oprF$) without (white) and with (gray) 0.5% arabinose (ara) in the indicated media. Error bars, SEM (n=3); asterisk over error bar, statistically different from WT in the same medium (P < 0.05, two-way ANOVA with *post hoc* Bonferroni). Statistical difference between $\Delta oprF$ strains in different media are indicated by a bar and asterisk. (B and C) Biofilm formation of $\Delta oprF$ strain in variations of TSB and LB: unaltered, altered NaCl concentrations, altered glucose concentrations, and altered K_2 HPO $_4$ concentrations (left to right). Biofilm formation in each medium; error bars, SEM (n=3); asterisk over error bar, statistically different from $\Delta oprF$ in the original medium (P < 0.05, two-way ANOVA with *post hoc* Bonferroni). Dot, each biological replicates, which is the average of 6 technical replicates. See Fig. S5 and Table S2 and S3 for full comparisons.

strain when 0.5% arabinose was added. To determine if the $\Delta oprF$ biofilm defect in TSB exists in other *P. aeruginosa* strains, we constructed $\Delta oprF$ mutants in three other backgrounds: the tomato plant isolate E2, the water isolate MSH10, and the UTI isolate X24509 (25). Similar to PAO1, biofilm defects were observed in all three $\Delta oprF$ mutants when grown in TSB (Fig. S4A). Furthermore, the established oprF interruption mutant strain H636, which is made from an H103-based PAO1 background (26), exhibited a significant biofilm defect when grown in TSB (Fig. S4B). However, in agreement with a previously published study (13), the H636 strain produced approximately double the biofilm biomass as the H103 parental strain in LB (Fig. S4C). This H636 result conflicts with our $\Delta oprF$ strain biofilm phenotype in LB (Fig. 1A), suggesting that the interruption mutation of oprF in H636 may be polar or that

the H636 strain may have acquired secondary mutations. Nonetheless, since all $\Delta oprF$ strains that we tested had a biofilm defect in TSB, we continued our studies using our *P. aeruginosa* PAO1 $\Delta oprF$ strain.

Glucose and low sodium chloride reduce *AoprF* biofilm formation. While TSB and LB are both rich media with peptic digests as primary carbon sources, three notable ingredients differ between the two: sodium chloride (NaCl), glucose, and dipotassium phosphate (K_2HPO_4) (Table S1). To determine if these media components affect $\Delta oprF$ biofilm formation, we measured the static biofilm formed when strains were grown in media in which the concentrations of these components were individually altered to match that of the other medium. First, biofilms were grown in TSB or LB, each containing 5 or 10 g/L NaCl. Since reducing the NaCl concentration below 5 g/L decreases cell viability in oprF mutants (27), we did not test sodium chloride concentrations below this threshold. While $\Delta oprF$ formed less biofilm than wild type in TSB (with 5 g/L NaCl; original formula), $\Delta oprF$ formed biofilms similar to those of wild type when the NaCl concentration was increased to 10 g/L (with no other change in TSB) (Fig. 1B and S5A). The reciprocal effect was observed with LB, where $\Delta oprF$ formed biofilms similar to wild type in the original medium (with 10 g/L NaCl) but less biofilm than wild type when NaCl was reduced to 5 g/L (Fig. 1C and S5A). This reduced biofilm formation mirrors $\Delta oprF$ biofilms formed in TSB, which also contains 5 g/L NaCl. Changing the glucose concentration had a similar effect. Removing glucose from TSB resulted in $\Delta oprF$ biofilm biomass similar to that of wild type (Fig. 1B and S5B), mirroring the phenotype of $\Delta oprF$ biofilms formed in LB, which does not contain glucose (Fig. 1C and S5B). When glucose was added to LB, $\Delta oprF$ formed less biofilm than wild type, similar to the biofilm formed by the mutant in TSB (which contains glucose). Changing the amount of K_2HPO_4 did not change the $\Delta oprF$ biofilm phenotype in either medium (Fig. 1B and C and Fig. S5C). These biofilm phenotypes were not the result of growth defects, as the planktonic growth rates of wild-type and $\Delta oprF$ strains in these altered media were statistically equivalent (Fig. S2). These results indicate that $\Delta oprF$ biofilm formation is dependent on the NaCl and alucose concentrations.

ΔoprF biofilm phenotype is not due to changes in osmolarity or metal concentrations. Since altering concentrations of major solutes may affect medium osmolarity, we tested if the medium osmolarity is related to the $\Delta oprF$ biofilm defect by measuring the osmolarity of the various TSB and LB media with a vapor pressure osmometer and then correlating these measurements to the amounts of $\Delta oprF$ static biofilm biomass formed in the media. While there was a weak positive correlation between media osmolarity and $\Delta oprF$ biofilm formation, the relationship was not statistically significant (Fig. S6). We noted that the effect of osmolarity appeared to be driven by the changes in sodium chloride concentration within each medium (Fig. S6, squares). In comparison, glucose, which impacted $\Delta oprF$ biofilm formation, did not alter media osmolarity (Fig. S6, triangles). Assuming that these medium components impact biofilm formation through the same mechanism, we conclude that changes in osmolarity are not the major driving force behind the effect on $\Delta oprF$ biofilm formation.

Changes to media formulations can also affect the concentrations of biologically relevant metals. To determine the concentrations of iron, manganese, nickel, cobalt, copper, molybdenum, sodium, potassium, magnesium, calcium, and zinc, we performed inductively coupled plasma mass spectrometry (ICP-MS) for each base medium and variant. While concentrations of sodium and potassium were altered when changes were made to sodium chloride or dipotassium phosphate, metal concentrations were primarily tracked with TSB or LB base media (Fig. S7). Furthermore, there was no significant correlation between individual metal concentrations and $\Delta oprF$ biofilm formation (P > 0.05, Pearson's coefficient). These results suggest that the nutrient-dependent effect of OprF in biofilm formation is not due to differential metal concentrations.

OprF affects late-stage biofilms in TSB. The nutrient-dependent effects of OprF detailed above occurred in biofilms grown for 24 h. To pinpoint the potential time-dependent effects of OprF in biofilm formation, we performed static microtiter biofilm assays in TSB for 1, 4, 8, 16, and 24 h (28). There was no defect in the attached biomass of $\Delta oprF$ relative to that of wild type at any time point between 1 and 16 h (Fig. 2). Unexpectedly, at 8 h, $\Delta oprF$ formed more biofilm than wild type in TSB (Fig. 2C). However, by the 16-h time point, $\Delta oprF$ biofilm

Month YYYY Volume XX Issue XX 10.1128/jb.00080-23

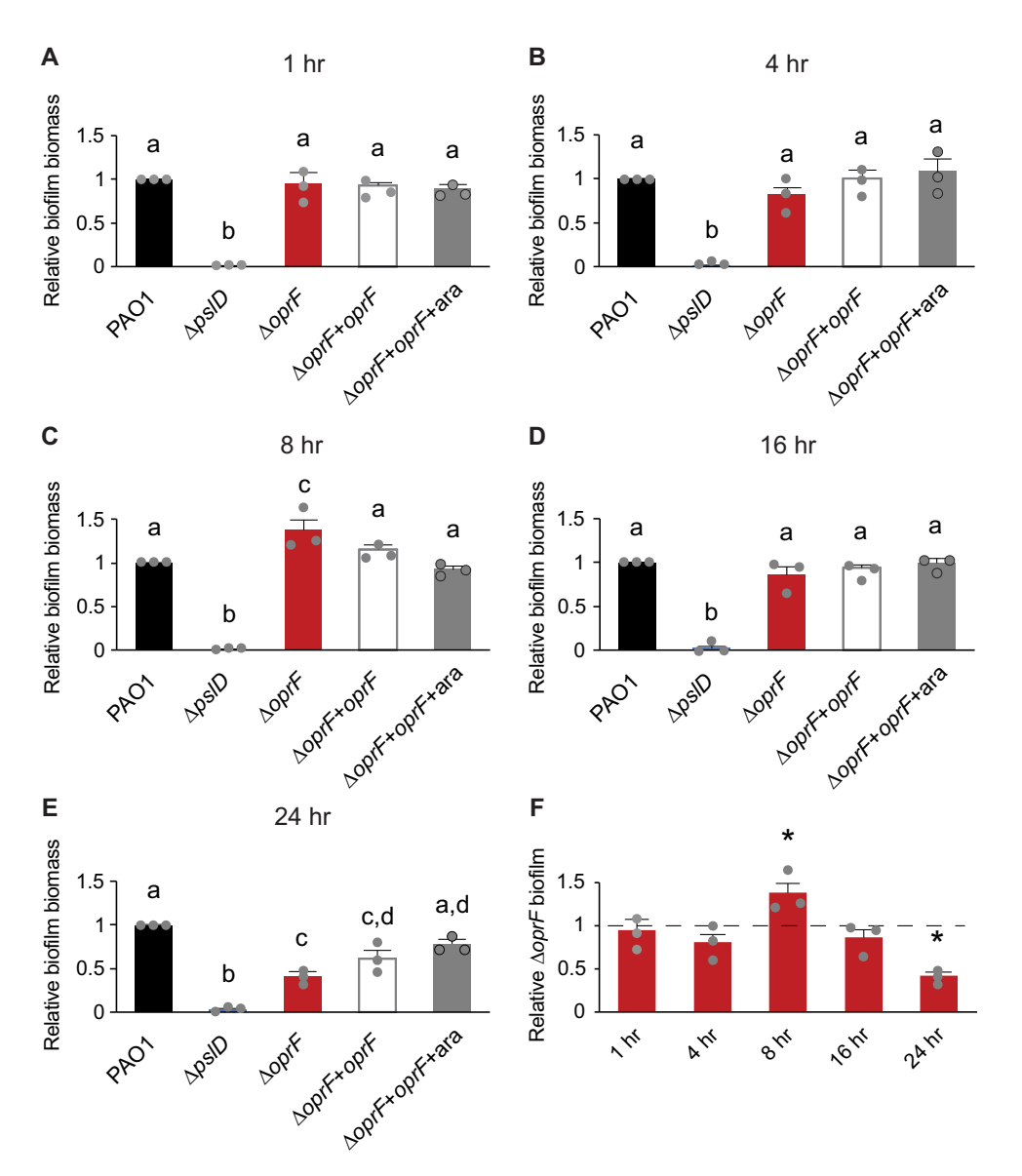


FIG 2 OprF affects late-stage biofilms in TSB. (A) 1-h static microtiter biofilm assays were performed in TSB with PAO1 (WT, black), $\Delta psID$ (blue), $\Delta oprF$ (red), and a $\Delta oprF$ attTn7::P_{BAD}-oprF restoration strain ($\Delta oprF + oprF$) with (white) and without (gray) 0.5% arabinose (ara). (B to E) 4-h (B), 8-h (C), 16-h (D), and 24-h (E) assays were performed with the same strains and media. (F) Static $\Delta oprF$ biofilm formation relative to WT (dashed line) at respective time points is represented. Biofilm formation is normalized to WT in each respective medium. Error bars, SEM (n = 3); dot, each biological replicate, which is the average of 3 to 6 technical replicates; letters, statistical groupings (P < 0.01, one-way ANOVA with post hoc Tukey HSD); asterisk, statistically different from WT at the same time point.

levels once again matched those of wild type (Fig. 2D). These results suggest that the $\Delta oprF$ defect does not begin in the early stages of static biofilm formation. Instead, between the 16-h and 24-h time points, $\Delta oprF$ static biofilm biomass decreased by 36.8 \pm 9.0% SD (n=3), while wild type increased 27.1 \pm 16.1% SD (n=3). This suggests that without OprF the static biofilm cannot maintain its biomass in TSB. Investigation of biofilm maintenance is ideally performed under continuous media flow, as it allows the biofilm to form for several days (29). However, the $\Delta oprF$ strain does not form biofilms on glass slides under media flow (E. K. Cassin and B. S. Tseng, unpublished data), limiting our methods to static assays. Combined with our earlier data on the nutrient-dependent effects of OprF, these data suggest that OprF is involved in the maintenance of P. aeruginosa biofilms in the presence of glucose or low sodium chloride.

The $\Delta oprF$ TSB biofilm defect is not dependent on PQS biosynthesis. The role of OprF in late-stage biofilm formation is interesting because planktonic oprF mutants make

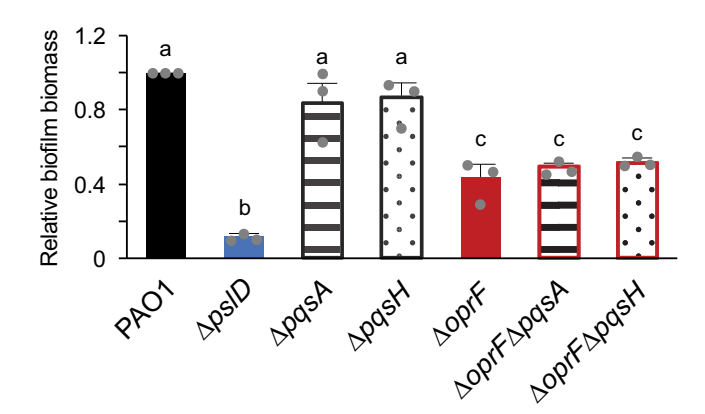


FIG 3 $\Delta oprF$ biofilm defect in TSB is independent of PQS. The 24-h static microtiter biofilm assays were performed in TSB with PAO1 (black), $\Delta psID$ (blue), $\Delta pqsA$ (stripes), $\Delta pqsH$ (dots), $\Delta oprF$ (red), $\Delta oprF\Delta pqsA$ (stripes with red outline), and $\Delta oprF\Delta pqsH$ (dots with red outline). Biofilm formation is normalized to WT. Error bars, SEM (n=3); dot, each biological replicate, which is the average of 4 technical replicates; letters, statistical groupings (P<0.01, one-way ANOVA with post hoc Tukey HSD).

more OMVs than wild-type cells and OMV production increases just before dispersal (22, 23). We hypothesized that the $\Delta oprF$ biofilm defect in TSB may be due to an increased OMV production, resulting in dispersion and less biofilm biomass relative to wild type. Since the increased OMV production of oprF mutants is due to PQS overproduction and deletion of PQS biosynthesis genes in an oprF mutant significantly decreases OMV production (22), we tested if deleting pqsA or pqsH in the $\Delta oprF$ strain would rescue the $\Delta oprF$ biofilm defect in TSB. Since PqsA is involved in the first steps of PQS biosynthesis and PqsH in the final step, a $\Delta oprF\Delta pqsA$ strain does not produce PQS or the PQS precursor HHQ, while a $\Delta oprF\Delta pqsH$ strain produces HHQ but not PQS (30). While the $\Delta pqsA$ and $\Delta pqsH$ single deletion strains formed biofilms equal to wild type, both $\Delta oprF\Delta pqsA$ and $\Delta oprF\Delta pqsH$ formed biofilms equivalent to those of $\Delta oprF$ in TSB (Fig. 3), suggesting that increased PQS, and thereby OMV production, from the $\Delta oprF$ mutant strain is not responsible for the biofilm defect in TSB.

Description Description D titer biofilm assays use crystal violet to stain surface-attached biomass as a proxy for total biofilm formation (28). Since crystal violet stains many biofilm components, including biofilm cells and the extracellular matrix, it is an indiscriminate indicator of surface-attached biomass. Therefore, we performed biofilm cell viability assays (28) in tandem with microtiter biofilm assays to tease apart which major components of the biofilm are affected by OprF. Surprisingly, despite the 60% decrease in total biofilm biomass in a side-by-side crystal violet staining (Fig. 4A), $\Delta oprF$ static microtiter biofilms in TSB contain approximately the same number of cells as that of wild type (Fig. 4D). As anticipated for static $\Delta oprF$ biofilms grown in LB (Fig. 4B) and TSB with 10 g/L NaCl (Fig. 4C), which do not exhibit a static biofilm defect, there is no statistical difference between the number of $\Delta oprF$ and wild-type biofilm cells (Fig. 4E and F, respectively). Furthermore, to verify that the 60% decrease in $\Delta oprF$ static biofilms was not due to differential crystal violet staining between strains, we stained planktonic wild-type and $\Delta oprF$ cells. These strains stain equivalently with crystal violet at the cell densities observed in the biofilm cell viability assays (Fig. S8). These results suggest that $\Delta oprF$ static biofilms in TSB contain less matrix, while biofilm cells remain attached to the surface, and that OprF is involved in maintaining or retaining the biofilm matrix.

ΔoprF biofilms in TSB contain less eDNA than wild-type biofilms. Since crystal violet stains negatively charged molecules, we reasoned that less eDNA in the biofilm could result in less stained biofilm biomass in the static biofilm assays. To quantify the eDNA in ΔoprF biofilms, we grew static ΔoprF or wild-type biofilms in TSB, LB, or TSB with 10 g/L NaCl and stained them with the eDNA-specific fluorophore DiTO-1. Static ΔoprF biofilms grown in TSB exhibit more eDNA-associated signal than the ΔpslD biofilm-negative-control strain, but 58.6 \pm 4.5% SD (n = 3) less eDNA signal than wild-type biofilms (Fig. 5A). This significant defect suggests that in the absence of OprF, eDNA is lost from the biofilm matrix. The lack of

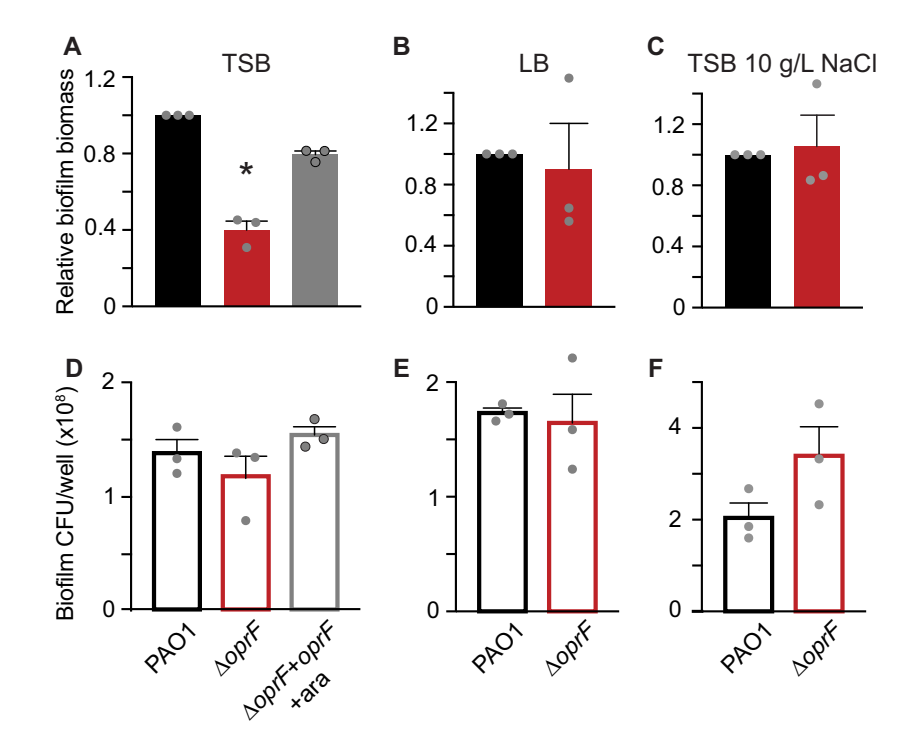


FIG 4 $\Delta oprF$ exhibits no biofilm cell viability defect in TSB. Side-by-side 24-h static microtiter biofilms (A to C, solid bars) and biofilm cell viability assays (D to F, outlined bars) were performed in the same 96-well plate with *P. aeruginosa* PAO1 (WT, black), $\Delta oprF$ (red), and the $\Delta oprF$ $attTn7::P_{BAD}$ -oprF restoration strain with 0.5% arabinose ($\Delta oprF + oprF +$ ara; gray). Biofilms were grown in TSB (A and D), LB (B and E), or TSB with 10 g/L NaCl (C and F). Static biofilm formation (A to C) is normalized to WT. Error bars, SEM (n=3); dot, each biological replicate, which is the average of 5 technical replicates; asterisks, statistical difference from PAO1 (P < 0.05, one-way ANOVA with $post\ hoc$ Tukey HSD).

a significant effect on eDNA levels in biofilms grown in LB or TSB with 10 g/L NaCl demonstrates that OprF affects eDNA in a nutrient-dependent manner (Fig. 5B and C). When combined with our earlier results, these results suggest that under certain conditions, OprF is involved in retaining eDNA in the *P. aeruginosa* biofilm matrix.

DISCUSSION

Our results highlight that growth conditions, specifically glucose and sodium chloride concentrations, impact *P. aeruginosa oprF* mutant biofilm phenotypes. *P. aeruginosa \Delta oprF* strains formed significantly less biofilm in TSB than LB. The decrease in $\Delta oprF$ biofilm in TSB

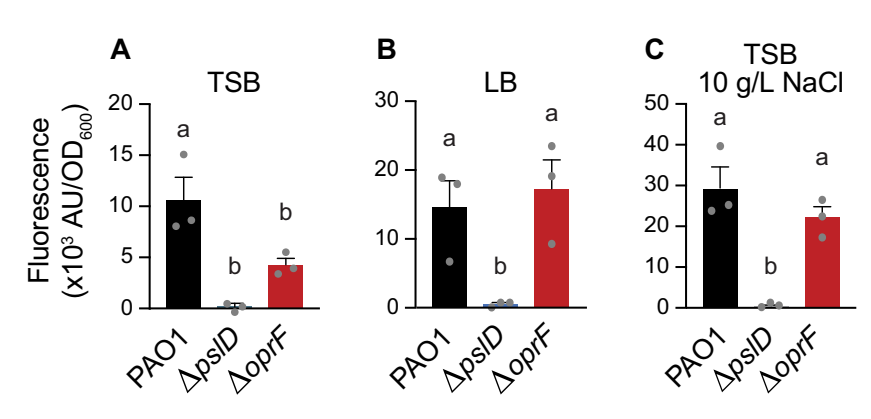


FIG 5 OprF affects biofilm eDNA levels in TSB. 24-h static microtiter PAO1 (black), $\Delta psID$ (blue), and $\Delta oprF$ (red) biofilms grown in TSB (A), LB (B), or TSB (C) with 10 g/L NaCl were stained with the eDNA-specific dye DiTO-1. Fluorescence intensity from each strain was normalized to respective biofilm cell numbers (via absorbance at OD₆₀₀). Error bars, SEM (n=3); dot, each biological replicate, which is the average of 5 technical replicates; letters, statistical groupings (P<0.05, one-way ANOVA with post hoc Tukey HSD).

occurred between 16 and 24 h and did not result in fewer P. aeruginosa cells. Instead, $\Delta oprF$ biofilms in TSB contained significantly less eDNA than wild-type biofilms. The mechanisms underlying how glucose and low sodium chloride led to decreased biofilms in cells lacking OprF is an exciting topic for future studies, as is determining how matrix-associated OprF affects eDNA levels.

Bouffartigues and colleagues previously found that an oprF interruption mutant forms approximately twice as much biofilm as the parental strain in LB, suggesting that a lack of OprF results in biofilm overproduction (13). Our results in LB using the same oprF interruption mutant strain agree with this conclusion. While these results follow the overall trend we saw in our $\Delta oprF$ strain in TSB and LB (Fig. 1), we did not observe hyperbiofilm formation in our $\Delta oprF$ strain in LB. Since both strains are of the PAO1 lineage and whole-genome sequencing of our $\Delta oprF$ strain confirmed that no other differences exist between this strain and the parental, the difference in biofilm phenotypes suggests that there may be additional genetic factors at play. It is possible that the insertion in oprF in H636 affects biofilm formation or that the strain has accumulated secondary mutations within or outside the oprF interruption that affect biofilm formation in LB. These possibilities could be sorted out via future whole-genome sequencing of H636 and comparing it to its parental strain.

Matrix-associated OprF, a membrane protein containing many hydrophobic residues, is abundant in biofilm membrane vesicles (4, 5). OMV production in biofilms is dependent on PQS production (31), but in our experiments, abolishing PQS production did not impact the $\Delta oprF$ biofilm phenotype (Fig. 3). In a wild-type biofilm, cells produce OMVs via the bilayer couple model with PQS, and MVs via explosive cell lysis (31). In $\Delta pqsA$ biofilms, MVs are still produced (31), and we saw no defect in biofilm formation (Fig. 3). Similarly, MVs are likely still produced by cell lysis in the defective biofilms of both the $\Delta oprF$ and $\Delta oprF\Delta pgs$ strains. Notably, these mutant strains would produce vesicles with no OprF. Given that these strains exhibit 60% less biofilm than wild type, we conclude that this decline is due to the lack of OprF, independent of OMV production. Overall, the results of the current study indicate that in a $\Delta oprF$ background, PQS-mediated OMV synthesis is not related to the decrease in biofilm observed in TSB, which raises several questions outside the scope of this study: (i) do $\Delta oprF$ mutants in a biofilm produce more OMVs, as has been reported for planktonic oprF mutants (22); (ii) is matrix-associated OprF found only in vesicles; and (iii) how do glucose and low sodium chloride affect the typical functions of OprF in biofilms? Further research probing these questions would expand our understanding of the roles of OprF and OmpA homologs in biofilm matrices.

OprF significantly affects the P. aeruginosa biofilm when grown under certain conditions. It is tempting to assume that the 60% decline in $\Delta oprF$ biofilms grown in TSB (Fig. 4A) is a proportional loss of all biofilm components. However, the static microtiter biofilm assay quantifies total biomass with crystal violet that stains the negatively charged components of the biofilm, namely, cell surfaces, matrix membrane vesicles, and eDNA. Our biofilm cell viability assays demonstrate that $\Delta oprF$ biofilms do not lose 60% of their cells (Fig. 4B). Instead, the $\Delta oprF$ biofilms grown in TSB contain approximately 60% less eDNA than wild-type biofilms (Fig. 5A). eDNA is an essential P. aeruginosa matrix component primarily produced by biofilm cell lysis (21, 32). It has been proposed that membrane vesicles stabilize the matrix of wild-type biofilms through their interactions with eDNA (33). Therefore, OprF, which is abundant in membrane vesicles, may be involved, directly or indirectly, in these eDNA interactions and thereby in biofilm structural maintenance.

The maintenance of mature biofilms as an active, discrete stage in the biofilm life cycle has been a recent topic of discussion (29). In this model, established biofilms respond to environmental changes to persist as a community. In a static microtiter biofilm, these changes include depletion of nutrients and waste accumulation over time. Our data indicate that OprF affects static biofilms in TSB, with the established $\Delta oprF$ biofilm decreasing between 16 and 24 h of incubation. This phenotype suggests that in the absence of OprF, biofilm formation progresses and subsequently degrades. When combined with our biofilm cell viability results (Fig. 4), $\Delta oprF$ biofilm degradation does not appear to be due to dispersion since cell numbers are maintained. Therefore, we hypothesize that OprF may be involved in matrix

retention in static biofilm maintenance via (i) matrix-bound OprF interactions with eDNA or (ii) intracellular regulatory effects of deleting *oprF*. Future research into these lines of questioning is necessary and will contribute to an expanded understanding of the role of OprF in biofilm maintenance.

MATERIALS AND METHODS

Bacterial strains and growth conditions. Bacterial strains, oligonucleotides, and plasmids used in this study are in Tables S4-S6. Strains produced for this study were constructed using allelic exchange, as in reference 34 and described in Supplemental Methods. Liquid lysogeny broth (LB) and tryptic soy broth (TSB) were prepared according to the recipe in Table S1. The PAO1 $\Delta oprF + oprF$ strain containing oprF under an arabinose-inducible promoter was grown in media containing 0.5% ι -arabinose (Sigma-Aldrich). Unless otherwise noted, strains were grown at 37°C in specified media with 250 RPM shaking or on semisolid LB containing 1.5% Bacto agar.

Static microtiter biofilm assays. Static biofilms were grown as described in (24). Overnight cultures of bacteria grown in appropriate media were diluted 1:100, and 100 μ L was seeded into sterile round-bottom 96-well polystyrene plates (Greiner Bio-One; no. 650101). Plates were incubated at 37°C without shaking for the indicated time. Planktonic cells were removed by triplicate washes in deionized water. Attached biofilm biomass was stained with 0.1% crystal violet for 15 min and washed as above. Stained biomass was solubilized using 30% acetic acid and transferred to a flat-bottom 96-well plate (Greiner Bio-One; no. 655090), and the absorbance at optical density at 550 nm (OD₅₅₀) was read in a Synergy Hybrid HTX Microplate Reader (BioTek Instruments). Absorbance from blank media wells was subtracted from raw OD₅₅₀ readings. Absorbance value of each strain was normalized to the average absorbance of the wild-type or parental strain. Three to six technical replicates within each biological replicate were averaged, and the average measurement of three biological replicates was used to statistically compare biofilm formation by one-way ANOVA with *post hoc* Tukey honestly significant difference (HSD) for assays with one independent variable or two-way ANOVA with *post hoc* Bonferroni Correction for assays with two independent variables. All statistical analyses were performed in IBM SPSS.

Biofilm cell viability assays. Biofilms were grown as above in static microtiter biofilm assays. Following incubation, planktonic cells were removed by washing with sterile deionized water poured over plates three times. Half of the wells in each plate were scraped with sterile flat toothpicks in 125 μ L sterile PBS to remove attached biofilm biomass. Solubilized biomass was serially diluted, spread on LB agar, and incubated at 37°C. CFU/well (100 μ L/well) was enumerated after 24 h. The other half of the wells in each plate were stained with crystal violet, as detailed in static microtiter biofilm assays above. Five technical replicates within each biological replicate were averaged, and the average CFU/well of the three biological replicates was used to statistically compare cell counts by one-way ANOVA with *post hoc* Tukey HSD.

Biofilm eDNA fluorescence assays. Biofilms were grown as above in static microtiter biofilm assays in TSB, LB, or TSB with 10 g/L NaCl growth media. Following incubation, planktonic cells were removed by washing with sterile deionized water poured over plates three times. Half of the wells in the plate were stained with eDNA-specific DiTO-1 (1 μM; AAT Bioquest; no. 17575) for 15 min. Stain was removed by pipetting and each well was subsequently rinsed with 100 μL PBS in triplicate. Attached, stained biomass was removed by scraping with sterile toothpicks, as in biofilm cell viability assays above, each well containing 125 μL sterile PBS. Scraped, stained biomass was transferred to a flat-bottomed, black-walled 96-well plate (Greiner Cellstar; no. 655090) and the fluorescence (excitation, 485/20; emission, 528/20) and absorbance (OD₆₀₀) were measured in a Synergy Hybrid HTX Microplate Reader (BioTek Instruments). One-quarter of the unstained wells were processed for cell viability and one-quarter were processed for crystal violet staining to assess total biofilm formation, as above. The background fluorescent signal from wells incubated with media only was subtracted from total fluorescence, and the average total fluorescence from five technical replicates per biological replicate were averaged. The average fluorescence per biological replicate was normalized to the average OD₆₀₀ value per strain. The average fluorescence/OD₆₀₀ of the three biological replicates was used to statistically compare strain fluorescence by one-way ANOVA with *post hoc* Tukey HSD.

SUPPLEMENTAL MATERIAL

Supplemental material is available online only. **SUPPLEMENTAL FILE 1**, PDF file, 10.2 MB. **SUPPLEMENTAL FILE 2**, XLSX file, 0.1 MB.

ACKNOWLEDGMENTS

We thank Kenesha Rae Broom, Mia G. Bruce, and Lindsey O'Neal for technical assistance and Jeffrey W. Schertzer for critical discussions of this work.

This project is funded by the NIH (K22 Al121097, P20 GM103440) and the Human Frontier Science Program (RGY00080/2021). In addition, E.K.C., D.S.B., and M.C.L. were supported by NASA (80NSSC20M0043), S.A.A.-H, D.Q.R., and D.S.B. were supported by NSF (no. 1301726 and 1757316), and E.K.C. and M.C.L. were supported by University of Nevada Las Vegas Top Tier Doctoral Graduate Research Assistantships. A.P. was supported by NSF (no. 2033286).

We thank Linda Nikolova and David Belnap for assistance at the Electron Microscopy Core Laboratory of the University of Utah.

Month YYYY Volume XX Issue XX

Conceptualization: E. K. Cassin and B. S. Tseng; Formal Analysis, Investigation, Methodology, or Visualization of Data: E. K. Cassin, S. A. Araujo-Hernandez, D. S. Baughn, M. C. Londono, D.Q. Rodriguez, N. S. Al-Otaibi, A. Picard, J. R. C. Bergeron, and B. S. Tseng; Writing – Original Draft: E. K. Cassin, B. S. Tseng; and Writing – Review And Editing: E. K. Cassin, M. C. Londono, N. S. Al-Otaibi, A. Picard, J. R. C. Bergeron, and B. S. Tseng.

REFERENCES

- Costerton JW, Stewart PS, Greenberg EP. 1999. Bacterial biofilms: a common cause of persistent infections. Science 284:1318–1322. https://doi.org/10.1126/ science.284.5418.1318.
- Fong JNC, Yildiz FH. 2015. Biofilm matrix proteins. Microbiol Spectr 3:3.2.28. https://doi.org/10.1128/microbiolspec.MB-0004-2014.
- 3. Flemming HC, Wingender J. 2010. The biofilm matrix. Nat Rev Microbiol 8: 623–633. https://doi.org/10.1038/nrmicro2415.
- Toyofuku M, Roschitzki B, Riedel K, Eberl L. 2012. Identification of proteins associated with the Pseudomonas aeruginosa biofilm extracellular matrix. J Proteome Res 11:4906–4915. https://doi.org/10.1021/pr300395j.
- Couto N, Schooling SR, Dutcher JR, Barber J. 2015. Proteome profiles of outer membrane vesicles and extracellular matrix of pseudomonas aeruginosa biofilms. J Proteome Res 14:4207–4222. https://doi.org/10.1021/acs.jproteome .5b00312.
- Tseng BS, Reichhardt C, Merrihew GE, Araujo-Hernandez SA, Harrison JJ, MacCoss MJ, Parsek MR. 2018. A biofilm matrix-associated protease inhibitor protects pseudomonas aeruginosa from proteolytic attack. mBio 9: e00543-18. https://doi.org/10.1128/mBio.00543-18.
- Zhang W, Sun J, Ding W, Lin J, Tian R, Lu L, Liu X, Shen X, Qian PY. 2015. Extracellular matrix-associated proteins form an integral and dynamic system during Pseudomonas aeruginosa biofilm development. Front Cell Infect Microbiol 5:40. https://doi.org/10.3389/fcimb.2015.00040.
- Absalon C, Van Dellen K, Watnick PI. 2011. A communal bacterial adhesin anchors biofilm and bystander cells to surfaces. PLoS Pathog 7:e1002210. https://doi.org/10.1371/journal.ppat.1002210.
- Jiao Y, D'haeseleer P, Dill BD, Shah M, Verberkmoes NC, Hettich RL, Banfield JF, Thelen MP. 2011. Identification of biofilm matrix-associated proteins from an acid mine drainage microbial community. Appl Environ Microbiol 77:5230–5237. https://doi.org/10.1128/AEM.03005-10.
- Wu S, Baum MM, Kerwin J, Guerrero D, Webster S, Schaudinn C, VanderVelde D, Webster P. 2014. Biofilm-specific extracellular matrix proteins of nontypeable Haemophilus influenzae. Pathog Dis 72:143–160.
- Cassin EK, Tseng BS. 2019. Pushing beyond the envelope: the potential roles of OprF in Pseudomonas aeruginosa biofilm formation and pathogenicity. J Bacteriol 201:e00050-19. https://doi.org/10.1128/JB.00050-19.
- Yoon SS, Hennigan RF, Hilliard GM, Ochsner UA, Parvatiyar K, Kamani MC, Allen HL, DeKievit TR, Gardner PR, Schwab U, Rowe JJ, Iglewski BH, McDermott TR, Mason RP, Wozniak DJ, Hancock RE, Parsek MR, Noah TL, Boucher RC, Hassett DJ. 2002. Pseudomonas aeruginosa anaerobic respiration in biofilms: relationships to cystic fibrosis pathogenesis. Dev Cell 3: 593–603. https://doi.org/10.1016/s1534-5807(02)00295-2.
- Bouffartigues E, Moscoso JA, Duchesne R, Rosay T, Fito-Boncompte L, Gicquel G, Maillot O, Bénard M, Bazire A, Brenner-Weiss G, Lesouhaitier O, Lerouge P, Dufour A, Orange N, Feuilloley MG, Overhage J, Filloux A, Chevalier S. 2015. The absence of the Pseudomonas aeruginosa OprF protein leads to increased biofilm formation through variation in c-di-GMP level. Front Microbiol 6:630. https://doi.org/10.3389/fmicb.2015.00630.
- Song F, Wang H, Sauer K, Ren D. 2018. Cyclic-di-GMP and oprF are involved in the response of Pseudomonas aeruginosa to substrate material stiffness during attachment on polydimethylsiloxane (PMS). Front Microbiol 9:110. https:// doi.org/10.3389/fmicb.2018.00110.
- Chevalier S, Bouffartigues E, Bodilis J, Maillot O, Lesouhaitier O, Feuilloley MGJ, Orange N, Dufour A, Cornelis P. 2017. Structure, function and regulation of Pseudomonas aeruginosa porins. FEMS Microbiol Rev 41:698–722. https://doi.org/10.1093/femsre/fux020.
- Orme R, Douglas CW, Rimmer S, Webb M. 2006. Proteomic analysis of Escherichia coli biofilms reveals the overexpression of the outer membrane protein OmpA. Proteomics 6:4269–4277. https://doi.org/10.1002/pmic.200600193.
- Ma Q, Wood TK. 2009. OmpA influences Escherichia coli biofilm formation by repressing cellulose production through the CpxRA two-component system. Environ Microbiol 11:2735–2746. https://doi.org/10.1111/j.1462-2920.2009.02000.x.

- Gaddy JA, Tomaras AP, Actis LA. 2009. The Acinetobacter baumannii 19606 OmpA protein plays a role in biofilm formation on abiotic surfaces and in the interaction of this pathogen with eukaryotic cells. Infect Immun 77:3150–3160. https://doi.org/10.1128/IAI.00096-09.
- Schooling SR, Beveridge TJ. 2006. Membrane vesicles: an overlooked component of the matrices of biofilms. J Bacteriol 188:5945–5957. https://doi.org/10.1128/JB.00257-06.
- Schertzer JW, Whiteley M. 2012. A bilayer-couple model of bacterial outer membrane vesicle biogenesis. mBio 3:e00297-11. https://doi.org/10.1128/ mBio.00297-11.
- Turnbull L, Toyofuku M, Hynen AL, Kurosawa M, Pessi G, Petty NK, Osvath SR, Cárcamo-Oyarce G, Gloag ES, Shimoni R, Omasits U, Ito S, Yap X, Monahan LG, Cavaliere R, Ahrens CH, Charles IG, Nomura N, Eberl L, Whitchurch CB. 2016. Explosive cell lysis as a mechanism for the biogenesis of bacterial membrane vesicles and biofilms. Nat Commun 7:11220. https://doi.org/10.1038/ncomms11220.
- Wessel AK, Liew J, Kwon T, Marcotte EM, Whiteley M. 2013. Role of Pseudomonas aeruginosa peptidoglycan-associated outer membrane proteins in vesicle formation. J Bacteriol 195:213–219. https://doi.org/10.1128/JB.01253-12.
- Cooke AC, Florez C, Dunshee EB, Lieber AD, Terry ML, Light CJ, Schertzer JW. 2020. Pseudomonas quinolone signal-induced outer membrane vesicles enhance biofilm dispersion in Pseudomonas aeruginosa. mSphere 5:e01109-20. https://doi.org/10.1128/mSphere.01109-20.
- 24. O'Toole GA. 2011. Microtiter dish biofilm formation assay. J Vis Exp 47: 2437. https://doi.org/10.3791/2437.
- Wolfgang MC, Kulasekara BR, Liang X, Boyd D, Wu K, Yang Q, Miyada CG, Lory S. 2003. Conservation of genome content and virulence determinants among clinical and environmental isolates of Pseudomonas aeruginosa. Proc Natl Acad Sci U S A 100:8484–8489. https://doi.org/10.1073/pnas.0832438100.
- Woodruff WA, Hancock RE. 1988. Construction and characterization of Pseudomonas aeruginosa protein F-deficient mutants after in vitro and in vivo insertion mutagenesis of the cloned gene. J Bacteriol 170:2592–2598. https://doi.org/10.1128/jb.170.6.2592-2598.1988.
- Gotoh N, Wakebe H, Yoshihara E, Nakae T, Nishino T. 1989. Role of protein F in maintaining structural integrity of the Pseudomonas aeruginosa outer membrane. J Bacteriol 171:983–990. https://doi.org/10.1128/jb.171.2.983-990.1989.
- Merritt JH, Kadouri DE, O'Toole GA. 2005. Growing and analyzing static biofilms. Curr Protoc Microbiol Chapter 1:Unit 1B.1. https://doi.org/10.1002/ 9780471729259.mc01b01s00.
- 29. Katharios-Lanwermeyer S, O'Toole GA. 2022. Biofilm maintenance as an active process: evidence that biofilms work hard to stay put. J Bacteriol 204:e0058721. https://doi.org/10.1128/jb.00587-21.
- Mashburn LM, Whiteley M. 2005. Membrane vesicles traffic signals and facilitate group activities in a prokaryote. Nature 437:422–425. https://doi.org/10.1038/nature03925.
- Cooke AC, Nello AV, Ernst RK, Schertzer JW. 2019. Analysis of Pseudomonas aeruginosa biofilm membrane vesicles supports multiple mechanisms of biogenesis. PLoS One 14:e0212275. https://doi.org/10.1371/journal.pone.0212275.
- Whitchurch CB, Tolker-Nielsen T, Ragas PC, Mattick JS. 2002. Extracellular DNA required for bacterial biofilm formation. Science 295:1487. https://doi.org/10.1126/science.295.5559.1487.
- Schooling SR, Hubley A, Beveridge TJ. 2009. Interactions of DNA with biofilm-derived membrane vesicles. J Bacteriol 191:4097–4102. https://doi .org/10.1128/JB.00717-08.
- Hmelo LR, Borlee BR, Almblad H, Love ME, Randall TE, Tseng BS, Lin C, Irie Y, Storek KM, Yang JJ, Siehnel RJ, Howell PL, Singh PK, Tolker-Nielsen T, Parsek MR, Schweizer HP, Harrison JJ. 2015. Precision-engineering the Pseudomonas aeruginosa genome with two-step allelic exchange. Nat Protoc 10: 1820–1841. https://doi.org/10.1038/nprot.2015.115.